Potency and Selectivity of Trifluoroacetylimino and Pyrazinoylimino Nicotinic Insecticides and Their Fit at a Unique Binding Site Niche

Motohiro Tomizawa,[‡] Shinzo Kagabu,[§] Ikuya Ohno,[§] Kathleen A. Durkin,[||] and John E. Casida*[,‡]

Environmental Chemistry and Toxicology Laboratory, Department of Environmental Science, Policy, and Management, University of California, Berkeley, California 94720-3112, Department of Chemistry, Faculty of Education, Gifu University, Gifu 501-1193, Japan, and Molecular Graphics and Computational Facility, College of Chemistry, University of California, Berkeley, California 94720-1460

Received February 22, 2008

Neonicotinoid agonists with a nitroimino or cyanoimino pharmacophore are the newest of the four most important classes of insecticides. Our studies on the nicotinic receptor structure in the neonicotinoid-bound state revealed a unique niche of about 6 Å depth beyond the nitro oxygen or cyano nitrogen tip. The N-substituted imino pharmacophore was therefore extended to fill the gap. Excellent target site selectivity with high insecticidal activity and low toxicity to mammals were achieved rivaling those of the current neonicotinoid insecticides as illustrated here by 3-(6-chloropyridin-3-ylmethyl)-2-trifluoroacetyliminothiazoline and its pyrazinoylimino analogue.

Introduction

The nicotinic acetylcholine (ACh) receptor (nAChR[a]) is an important target of insecticides for crop protection and public health and of therapeutic agents for neurological dysfunction. Neonicotinoid insecticides such as imidacloprid (IMI) and thiacloprid (THIA) (Chart 1) are increasingly replacing organophosphorus compounds and methylcarbamates because of improved safety and effectiveness particularly due to the selection of resistant pest strains.[1,2] High neonicotinoid potency and selectivity toward the insect nAChR are ultimately attributable to the differential binding site interactions which have been mapped with mollusk ACh binding proteins (AChBPs)[3,4] as excellent structural surrogates for the extracellular ligand-binding domain of the nAChRs.[5,6] The IMI binding site is located at an interfacial region between the primary or (+)-face and the complementary or (−)-face subunits of the AChBP (corresponding to α and non-α subunits, respectively, of the nAChR) (Figure 1). The nitro oxygen or cyano nitrogen tip of IMI or THIA, respectively, H-bonds to the backbone HN of C190 and/or S189 on loop C of the primary subunit of AChBP.[3] The AChBP−IMI structure, fascinatingly, provides a space of approximately 6 Å depth that extends from the IMI nitro tip oxygen toward Q57 on loop D of the (−)-face subunit. Q57 of AChBP is spatially equivalent to R, K, or N of the insect nAChR β subunits, while T with a shorter side chain takes this position on the β2 subunit of the vertebrate neuronal nAChR.

The structural model for the AChBP−neonicotinoid complex[3] prompted the present study of selected ligands proposed to fit the loop D amino acid(s) in the insect nAChRs. We designed a series of prototype compounds with extended N-substituted imine substituents (pyrazinoylimine and trifluoroacetylimine) (Chart 1 and Figure 1), finally leading to candidate nicotinic insecticides with high potency and excellent target site selectivity rivaling those of the present neonicotinoids and other chemotypes of commercial insecticides.

Results and Discussion

Structure−Activity Relationships (SAR) at the Insect nAChR. Replacement of the nitro- or cyanoimino pharmacophore by extended substituents may provide point(s) for hydrogen acceptance and/or van der Waals (VDW) contacts at the targeted regional binding domain: i.e., loop D amino acid(s) on the complementary or β subunit of the insect nAChR. According to this hypothesis, phenyl, pyridine, and pyrazine derivatives (**1**−**7**) were prepared and binding affinities evaluated with *Drosophila* nAChR (Table 1). The affinity of the phenyl analogue (**1**) was 9.3- to 25-fold lower than that of the pyridine compounds (**2**−**4**). The 2,5-pyrazine analogue (**5**) showed the highest affinity similar to a pyridinylidene-2-pyrazinecarboxamide neonicotinoid derivative with an affinity 4-fold less than IMI.[7,8] The SAR clearly indicates that hydrogen-accepting nitrogen atom(s) plays a crucial role in recognition by the amino acid(s) at the binding domain. The pyrazine moiety with two nitrogen atoms provides two hydrogen-accepting points. Nitrogen at the 5-position (equivalent to that of 3-pyridine) is important, and one at the 2-position (corresponding to that of 2-pyridine) enhances the potency. The 4-chlorophenyl compound (**6**) had >250-fold lower activity than unsubstituted **1**, and similarly, the 6-chloro-3-pyridinyl analogue (**7**) had an 8.5-fold reduced affinity compared to the unsubstituted 3-pyridinyl compound (**3**), suggesting that chlorine provides spatial hindrance at the binding domain. Most interestingly, compounds **8** and **9** with a trifluoroacetyl substituent, providing both VDW-contacting and hydrogen-accepting abilities, gave high affinities.

Insecticidal Activities (Table 1). Adult female houseflies (*Musca domestica*) were used for quantitative evaluation of insecticidal activity. First, intrinsic activities [defined by intrathoracic injection into flies which are pretreated with a cytochrome P450 inhibitor (synergist)] of test compounds were compared with neonicotinoid insecticides IMI and THIA. Analogues with phenyl (**1**), pyrazine (**5**), chloropyridine (**7**), and trifluoroacetyl (**8**, **9**) substituents had moderate to high insecticidal activity, whereas the three pyridine isomers (**2**, **3**, **4**) with high nAChR affinity were not insecticidal, suggesting metabolic instability. Interestingly chloropyridine analogue **7**

* To whom correspondence should be addressed. Phone: 510-642-5424. Fax: 510-642-6497. E-mail: ectl@nature.berkeley.edu.

[‡] Department of Environmental Science, Policy, and Management, University of California.

[§] Gifu University.

[||] College of Chemistry, University of California.

[a] Abbreviations: AChBP, acetylcholine binding protein; IMI, imidacloprid; MD, molecular dynamics; nAChR, nicotinic acetylcholine receptor; THIA, thiacloprid; VDW, van der Waals.

10.1021/jm800191a CCC: $40.75
Published on Web 06/21/2008

Chart 1. Structures of Two Major Neonicotinoid Insecticides Imidacloprid (IMI) and Thiacloprid (THIA) with Nitro- and Cyanoimine Moieties, Respectively, and the N-Substituted Imino Analogues (**1**−**9**)

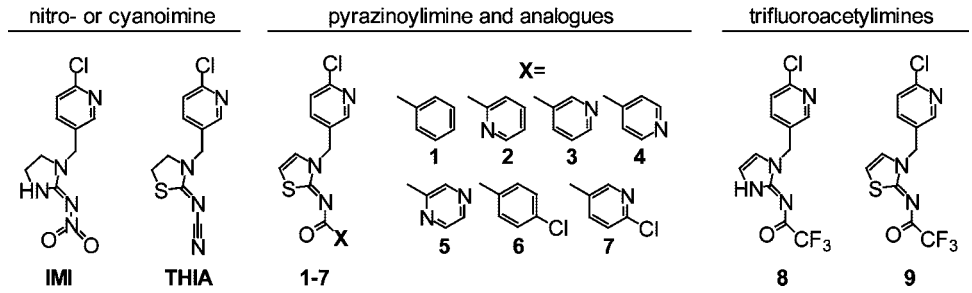

with moderate nAChR affinity was highly insecticidal, presumably conferring improved hydrophobicity and metabolic stability by introduction of the chlorine atom. In topical application, compounds **1** and **5** were quite potent with synergist, whereas **7**−**9** were as active as or more so than IMI and THIA. Remarkably, topically applied trifluoroacetyliminothiazoline **9** showed high insecticidal activity even in the absence of synergist, conceivably due to higher hydrophobicity and metabolic stability than those of IMI and THIA. More specifically, the activity level of **9** rivals those of other types of commercial insecticides (Table 1 footnote).

The common brown house mosquito (*Culex quinquefasciatus*) provides an example of a major pest with increasing difficulty to control because of selection of strains resistant to the major pyrethroid, organophosphate, and methylcarbamate insecticides. Neonicotinoids are possible replacements if they have suitable potency and little or no cross-resistance.[11,12] Neonicotinoid **9** was compared with permethrin, the standard mosquito control agent, for contact toxicity to adults and potency (50% lethal concentration or LC_{50}) on fourth instar larvae. Permethrin was far superior to **9** in contact adulticidal activity (data not shown). Although **9** was only 2.4-fold less active than permethrin as a larvicide on the susceptible colony, it was 6.7 times more potent on the permethrin-resistant colony (Table 2). The target site cross-resistance of pyrethroids and DDT or of organophosphates and methylcarbamates does not carry over to the neonicotinoids,[11,12] making them candidates for further development as mosquito control agents.

Selectivity. Selective toxicity is critical for insecticide use, combining outstanding effectiveness for pests with safety for humans and wildlife. The selectivity of representative compounds **5** and **9** was evaluated by comparing the binding affinity to the *Drosophila* and chick $\alpha4\beta2$ nAChRs and toxicity to houseflies and mice (Table 3). Relative to target site selectivity, compounds **5** and **9** had low potency at the chick $\alpha4\beta2$ nAChR (600- and 161-fold less active, respectively, than the insect

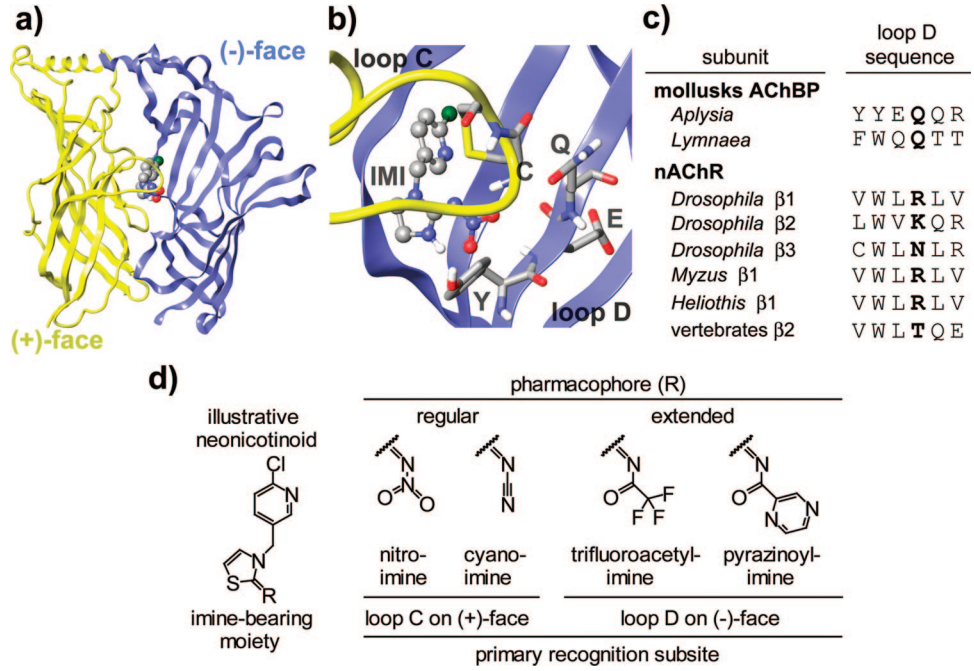

Figure 1. Design of selective nicotinic agonists interacting with loop D amino acid(s) in the insect nAChR. (a) IMI nestled in the interfacial agonist-binding pocket between the (+)-face (primary, yellow) and (−)-face (complementary, blue) subunits of the *Aplysia californica* AChBP[3] as a structural surrogate of the nAChR extracellular ligand-binding domain. (b) AChBP-IMI binding site interactions (zoomed-in) featuring hydrogen-bonding between the IMI nitro tip oxygen and the backbone HN of the loop C C190 and/or S189 (not shown, since it would obscure the nitro tip of IMI). An approximately 6 Å depth cavity exists beyond the nitro tip oxygen of IMI toward the loop D Q57 amide side chain. (c) Alignment of the loop D amino acid sequences from two mollusk AChBP subtypes, five insect β subunits (represented by fruit fly *Drosophila melanogaster*, peach−potato aphid *Myzus persicae*, and tobacco budworm *Heliothis virescens*) and the vertebrate (human, rodent, and chick) $\beta2$ subunit of the nAChR. (d) Selected prototype compounds with N-substituted imine moiety and extended pharmacophore replacing the regular nitro- or cyanoimine moiety. The trifluoroacetylimine or pyrazinoylimine is expected to undergo hydrogen-bonding and/or van der Waals (VDW) contacts with the loop D niche, whereas the nitro or cyano tip atom interacts primarily with the loop C region.

Table 1. SAR of Neonicotinoids in Terms of Insect nAChR Affinity and Insecticidal Activity

		LD_{50} (μg/g)[b,c]		
			topical	
compd[a]	IC_{50} ± SD (nM)[b,c]	injection synergist[d]	synergist[d]	alone[e]
Pyrazinoylimine and Analogues				
1	121 ± 6	1.0	2.0	>10 (0%)
2	13 ± 1	>1 (0%)	>10 (0%)	>10 (0%)
3	4.8 ± 0.2	>1 (13%)	>10 (0%)	>10 (0%)
4	10 ± 2	>1 (13%)	>10 (0%)	>10 (0%)
5	1.5 ± 0.04	0.035	2.8	>10 (0%)
6	>30000 (10%)	>1 (0%)	>10 (0%)	>10 (0%)
7	41 ± 2	0.080	0.12	>10 (0%)
Trifluoroacetylimine Analogues				
8	7.7 ± 0.7	0.064	0.071	~10
9	3.1 ± 1.0	0.027	0.035	0.75[f]
Nitro- and Cyanoimine Standards				
IMI	4.3 ± 0.3	0.021	0.20	>10 (0%)
THIA	2.7 ± 0.4	0.032	0.14	>10 (19%)

[a] Calculated log *P* values by ALOGPS[9] for compounds **1**−**9** are 3.56, 2.48, 2.21, 2.20, 1.61, 4.14, 3.35, 2.40, and 3.04, respectively, compared with those of IMI and THIA of 0.65 and 1.91 (observed log *P* of 0.57 and 1.26),[2] respectively. [b] Assayed as [^{3}H]IMI binding to the *Drosophila* nAChR and toxicity against adult female houseflies. [c] Percent inhibition or mortality at the indicated concentration or dose is given in parentheses. [d] Pretreated topically with the synergist *O*-propyl *O*-(2-propynyl)phenylphosphonate (PPP) (100 μg/g) before administration of the test chemical. [e] Standard insecticides chlorpyrifos and propoxur gave LD_{50} of 2.1 and 37 μg/g, respectively (present study), compared with those of parathion, propoxur, dieldrin, and DDT of 1.3, 23, 0.7, and 14 μg/g, respectively.[10] [f] Contact toxicity in the absence of metabolic inhibitor: dose for 50% knockdown, 0.04 μg/cm^2 (0.5−8 h); LD_{50}, 0.2 μg/cm^2 (24 h).

Table 2. Mosquito Larvicidal Activity of Neonicotinoid **9** and Permethrin with Susceptible and Permethrin-Resistant Colonies of Fourth Instar *Culex quinquefasciatus*

	LC_{50} (ppm)	
insecticide	susceptible	resistant
9	0.012	0.024[b]
permethrin[a]	0.0050	0.16

[a] 1-*RS*-Permethrin (trans ≤ 65% and cis ≥ 35%). [b] Estimated from a separate experiment showing that the resistant colony was 2-fold less sensitive than the susceptible colony.

Table 3. Selectivity between Insects and Vertebrates in Terms of nAChR Affinity and Organismal Toxicity

	IC_{50} ± SD (nM)			LD_{50} (mg/kg)		
compd[a]	*Drosophila*[b]	chick α4β2[c]	ratio	housefly[b]	mouse[d]	ratio
5	1.5 ± 0.04	900 ± 96	600	0.035	>24 (0%)[d]	>685
9	3.1 ± 1.0	500 ± 100	161	0.027	>36 (0%)[d]	>1333
IMI	4.3 ± 0.3	2600 ± 85	605	0.021	45	2142
THIA	2.7 ± 0.4	860 ± 31	319	0.032	28	875

[a] IC_{50} values (nM) of compounds **5** and **9** as displacers of [^{3}H]IMI binding to the hybrid nAChR consisting of peach−potato aphid (*M. persicae*) α2 and rat β2 subunits are 720 ± 46 and 280 ± 24, respectively, compared with those of IMI and THIA (3.6 ± 0.1 and 11 ± 1 nM, respectively).[13] [b] Data from Table 1 (binding affinity assayed with [^{3}H]IMI and insecticidal activity with synergist via injection). [c] Assayed with [^{3}H]nicotine. [d] Intraperitoneal administration. Percent lethality at the indicated dose (maximal dose administered because of the solubility limitation in vehicle) with no poisoning signs.

nAChR). Fascinatingly, at the organismal level, compounds **5** and **9** were >685- and >1300-fold less toxic to mice than houseflies. These intrinsic selectivity ratios at target site and toxicity levels were similar to those of IMI and THIA.[1,2] In addition, the binding affinities of **5** and **9** to a hybrid nAChR consisting of peach−potato aphid *Myzus persicae* α2 subunit and vertebrate (rat) β2 subunit were 720 and 280 nM, respectively (Table 3 footnote). In sharp contrast, insecticides IMI and THIA showed high affinities to the hybrid receptor (3.6 and 11 nM, respectively),[13] strongly indicating that the insect α subunit plays a critical role in the recognition of IMI and THIA with nitro- and cyanoimino moieties. However, the insect β subunit is presumably important for embracing the extended pyrazinoylimine or trifluoroacetylimine moiety of **5** or **9**.

Insect nAChR Binding Site Interactions. A structural model for the interfacial agonist-binding domain of the insect nAChR from *M. persicae* (α2β1) is established on the basis of the crystal structure of *Aplysia californica* AChBP, which is sensitive to neonicotinoids.[4] This model is representative of insect nAChRs, since the important amino acids forming the binding pockets are fully conserved in all of the known insect nAChRs. The AChBP molecular dynamics (MD) simulations defining the binding site interactions with **5** and **9** are given in Supporting Information as the foundation for those with the insect nAChR structural model.

In a MD snapshot for the insect nAChR liganded with pyrazinoylimine **5** (Figure 2), the pyrazine nitrogen atom at the 5-position H-bonds with the loop D R81 guanidine NH_2 (2.6 Å), although R81 may take multiple geometries because of its flexible carbon units. The N at the 2-position H-bonds with loop D W79 indole HN (2.2 Å), and the NC(O) oxygen makes contact with the W79 indole HN (2.6 Å). As with IMI and THIA,[3,4] the amidine plane π-stacks with the loop C Y224 aromatic residue (3−4 Å) and also with the loop B W174 side chain (4−5 Å). Similarly in a MD result for the complex with trifluoroacetylimine **9**, the three fluorine atoms variously interact with loops C and D: i.e., H-bonding to the backbone HN of C226 (2.4 Å) and V225 (3.3 Å) (not displayed), to R81 guanidine NH_2 (directly or possibly via a water bridge) (3.5 Å), and to W79 indole HN (2.5 Å). VDW contacts with the W79 indole ring. The NC(O) oxygen H-bonds to the W79 indole HN (2.7 Å). The amidine plane of **9** is sandwiched via π-stacking between the Y224 phenol ring (3−4 Å) and W174 indole residue (4−5 Å). For both compounds **5** and **9**, the chloropyridine Cl VDW-contacts to the backbone carbonyl oxygens of loops E N131 and L141 (3.3−3.7 and 3.2−3.4 Å, respectively) and the pyridine N undergoes H-bonding with the backbone carbonyl oxygens of loop E I143 and loop B W174 (4.3−4.4 and 3.9 Å, respectively) possibly via water bridge(s). Therefore, the pyrazinoyl (and possibly the pyridinoyl) moiety embraces primarily the loop D niche on the partnering subunit and the trifluoroacetyl substituent is nestled in an interfacial region between loops C and D, whereas the nitro- or cyanoimino pharmacophore of IMI or THIA principally interacts with the loop C tip area on the primary subunit. The present structural models are consistent with the observed SAR.

Target Site Selectivity. When the loop D regions on the β subunits from the insect (W79, L80, and R81) and vertebrate (W75, L76, and T77) receptors are overlaid, the insect R81 more intimately faces the pyrazine or CF_3 moiety compared to the vertebrate T77 (≥4 Å difference), presumably serving as a determinant for target site selectivity (Figure 3). Intriguingly, target site selectivity for IMI/THIA depends on multiple bound ligand conformations such that the final binding constant represents a combination of individual constants specific to different conformations; i.e., the weakly binding neonicotinoids adopt two different binding orientations at the vertebrate nAChR binding pocket, whereas a single tight binding conformation reflects the high affinity to the insect nAChR.[4] This unique

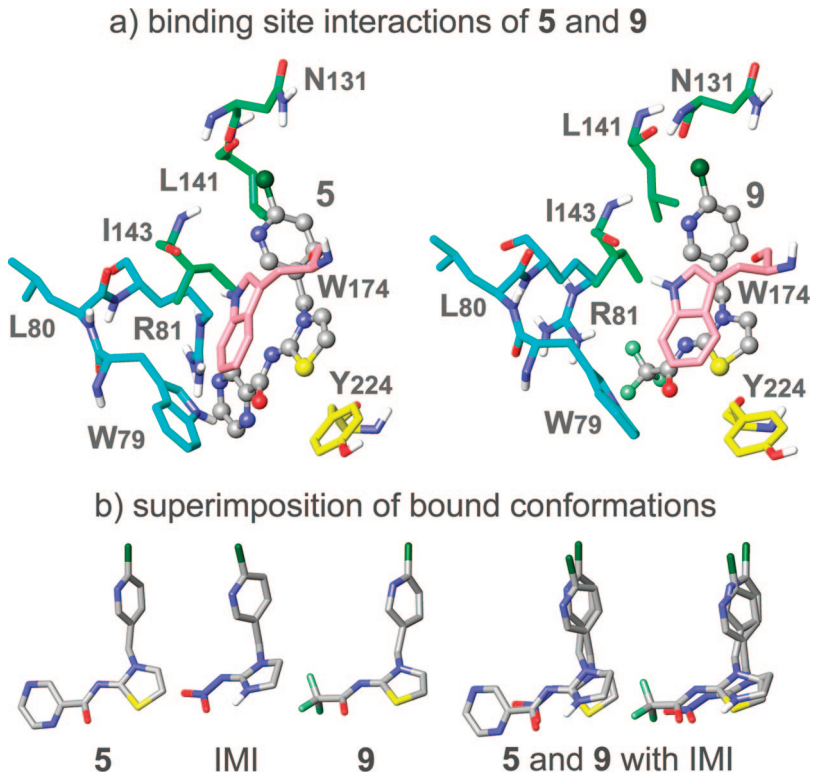

Figure 2. Structural models for binding site interactions of pyrazinoylimino (**5**) and trifluoroacetylimino (**9**) nicotinic insecticides with the α-β subunit interfacial agonist-binding domain of insect nAChR. (a) Relevant amino acids displayed are loop B W174 in pink; loop C Y224 in yellow; loop D W79, L80, and R81 in aquamarine; loop E N131, L141, and I143 in green. (b) Superimposition of bound conformation of **5** or **9** overlaid with that of IMI as observed in the insect receptor binding pocket.

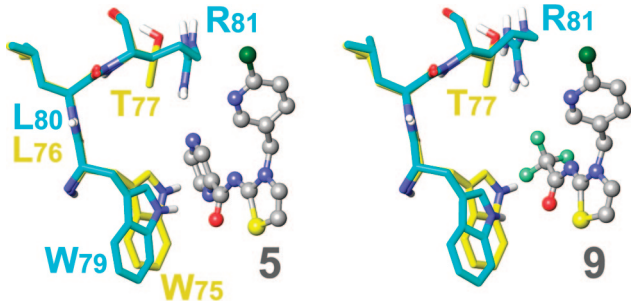

Figure 3. Structural comparison of loop D amino acids from insect and vertebrate β subunits with R81 and T77, respectively, suggesting their dissimilar interactions with **5** and **9**. Loop D amino acids W79, L80, and R81 (aquamarine) on the β subunit of the insect agonist-binding pocket (*Myzus* α2β1) interacting with **5** (left) or **9** (right) are superimposed onto the equivalent region W75, L76, and T77 (yellow) on the β subunit of the vertebrate (chick) α4β2 interface.[14]

concept may also be applicable to the present pyrazinoylimine and trifluoroacetylimine insecticides.

Concluding Remarks. Highly potent and selective nicotinic insecticides were achieved by pharmacophore modification of neonicotinoids with extended and hydrophobic substituents fitting the loop D amino acid(s) in the insect nAChR. The present investigation illustrates receptor structure-guided ligand design for lead generation and discovery of novel insecticides with excellent target site selectivity, high insecticidal activity, and low toxicity to mammals.

Experimental Section

General. 1-(6-Chloropyridin-3-ylmethyl)-2-trifluoroacetyliminoimidazoline (**8**) and its thiazoline analogue **9** were available from our previous studies.[15,16] All melting points (mp) are uncorrected. ^{1}H and ^{13}C NMR spectra were recorded for solutions in $CDCl_3$ unless otherwise stated using a JEOL ECA-500 spectrometer (Tokyo, Japan) at 500 and 125 MHz, respectively. Mass spectra were determined at 70 eV with the JEOL JMS-700 instrument. Combustion analyses were performed with the Yanaco CHN CORDER MT-6 elemental analyzer (Kyoto, Japan).

2-Benzoylimino-3-(6-chloro-3-pyridylmethyl)thiazoline (1), 2-(4-Chlorobenzoyl)imino-3-(6-chloro-3-pyridylmethyl)thiazoline (6), and 2-(6-Chloro-3-pyridinoyl)imino-3-(6-chloro-3-pyridylmethyl)thiazoline (7). To an ice-cooled solution of 3-[(6-chloro-3-pyridinyl)-methyl]-2-iminothiazoline[15,16] (113 mg, 0.5 mmol) and triethylamine (101 mg, 1 mmol) in pyridine (3 mL) was added slowly benzoyl chloride (77 mg, 0.55 mmol) (for compound **1**), 4-chlorobenzoyl chloride (180 mg, 1.03 mmol) (for compound **6**), or 6-chloro-3-pyridinoyl chloride (175 mg, 0.99 mmol) (for compound **7**). The reaction mixture was stirred at this temperature for 3.5 h, poured onto 20 mL of cold water, and alkalized to about pH 10 with Na_2CO_3. The resulting precipitate was filtered off, washed with water, and dried. Recrystallization from ethanol gave the products. Compound **1**: yield 45%; mp = 130 °C. ^{1}H NMR: δ 5.48 (s, 2H), 6.71 (d, 1H, J = 5.1 Hz), 7.02 (d, 1H, J = 5.1 Hz), 7.31 (d, 1H, J = 8.2 Hz), 7.43−7.52 (m, 3H), 7.70 (1H, dd, J = 8.2 Hz, 2.3 Hz), 8.30 (m,2H), 8.48 (d, 1H, J = 2.3 Hz). ^{13}C NMR: δ 48.7, 110.2, 124.9, 125.1, 128.3, 129.3, 130.5, 131.8, 136.6, 138.8, 149.2, 151.8, 168.2, 174.2. EI-LRMS m/z (%): 329 (M^+, 96), 293 (M^+ − Cl, 8), 224 (M^+ − COC_6H_5, 25), 188 (29), 126 (Cl − Py − CH_2, 36), 105 (COC_6H_5, 100). EI-HRMS calcd for $C_{16}H_{12}ClN_3OS$, 309.0390; found 309.0390. Anal. ($C_{16}H_{12}ClN_3OS$) calcd C, 58.27; H, 3.67; N, 12.74; found C, 57.97; H, 3.90; N, 12.74. Compound **6**: yield, 61%; mp = 191 °C. ^{1}H NMR: δ 5.48 (s, 2H), 6.74 (d, 1H, J = 4.8 Hz), 7.02 (d, 1H, J = 4.8 Hz), 7.32 (d, 1H, J = 8.2 Hz), 7.41 (d, 2H, J = 8.9 Hz), 7.68 (1H, dd, J = 8.2 Hz, 2.1 Hz), 8.23 (d, 2H, J = 8.9 Hz), 8.48 (d, 1H, J = 2.1 Hz). ^{13}C NMR: δ 48.7, 110.3, 124.9, 125.0, 128.4, 130.3, 130.6, 135.0, 137.9, 138.6, 149.1, 151.9, 168.2, 173.2. EI-LRMS m/z (%): 363 (M^+, 88), 293 (M^+ − Cl, 6), 224 (M^+ − COC_6H_5, 39), 188 (21), 139 (COC_6H_4Cl,

100), 126 (Cl − Py − CH_2, 46), 111 (C_6H_5Cl, 60). EI-HRMS calcd for $C_{16}H_{11}Cl_2N_3OS$, 363.0000; found 363.0014. Anal. ($C_{16}H_{11}Cl_2N_3OS$) calcd C, 52.76; H, 3.04; N, 11.54; found C, 52.56; H, 3.32; N, 11.34. Compound **7**: yield, 76%; mp = 176 °C. ^{1}H NMR: δ 5.48 (s, 2H), 6.80 (d, 1H, J = 4.6 Hz), 7.07 (d, 1H, J = 4.6 Hz), 7.33 (d, 1H, J = 8.2 Hz), 7.40(d, 1H, J = 8.3 Hz), 7.66 (dd, 1H, J = 8.2 Hz, 2.3 Hz), 8.44 (d, 1H, J = 2.3 Hz), 8.46 (dd, 1H, J = 8.3 Hz, 2.3 Hz), 9.24 (d, 1H, J = 2.3 z). ^{13}C NMR: δ 48.9, 110.7, 123.9, 124.8, 125.3, 129.9, 131.0, 138.5, 139.2, 149.0, 151.1, 152.0, 154.1, 168.2, 171.5. EI-LRMS *m*/*z* (%): 364 (M^+, 100), 293 (M^+ − Cl, 4), 224 (M^+ − COPy − Cl, 41), 208 (15), 188 (15), 140 (COPy − Cl, 93), 126 (Cl − Py − CH_2, 85), 112 (Py − Cl, 45). EI-HRMS calcd for $C_{15}H_{10}Cl_2N_4OS$, 363.9952; found 363.9948. Anal. ($C_{15}H_{10}Cl_2N_4OS$) calcd C, 49.33; H, 2.76; N, 15.34; found C, 49.02; H, 2.94; N, 15.25.

3-(6-Chloro-3-pyridylmethyl)-2-(2-pyridinoyl)iminothiazoline (2), 3-(6-Chloro-3-pyridylmethyl)-2-(3-pyridinoyl)iminothiazoline (3), 3-(6-Chloro-3-pyridylmethyl)-2-(4-pyridinoyl)iminothiazoline (4), and 3-(6-Chloro-3-pyridylmethyl)-2-(pyrazinoyl)iminothiazoline (5). To a solution of 3-[(6-chloro-3-pyridinyl)methyl]-2-iminothiazoline (75 mg, 0.25 mmol) and triethylamine (202 mg, 2.0 mmol) in acetonitrile (15 mL) was added slowly 2-pyridinoyl chloride hydrochloride (56 mg, 0.31 mmol) (for compound **2**), 3-pyridinoyl chloride hydrochloride (37 mg, 0.21 mmol) (for compound **3**), 4-pyridinoyl chloride hydrochloride (56 mg, 0.31 mmol) (for compound **4**), or pyrazinoyl chloride hydrochloride (50 mg, 0.28 mmol) (for compound **5**). The reaction mixture was stirred at the refluxing temperature for 4 h, and the solvent and excess triethylamine were removed in vacuo. The residue was taken up with ethyl acetate, washed successively with 10% aqueous Na_2CO_3 and water, and dried. Chromatography on silica with ethyl acetate and methanol (5:1) gave the products. Compound **2**: yield, 18%; mp = 207−208 °C. ^{1}H NMR: δ 5.51 (s, 2H), 6.73 (d, 1H, J = 4.1 Hz), 7.05 (d, 1H, J = 4.1 Hz), 7.27 (d, 1H, J = 8.3 Hz), 7.37 (m, 1H), 7.73(m, 1H), 7.79 (m, 1H), 8.29 (d, 2H, J = 8.3 Hz), 8.48 (d, 1H, J = 2.1 Hz), 8.76 (d, 1H, J = 4.2 Hz). ^{13}C NMR: δ 49.0, 110.7, 124.5, 124.8, 125.4, 125.6, 130.3, 136.7, 139.3, 149.6, 149.8, 151.8, 153.8, 169.0, 173.0. EI-LRMS *m*/*z* (%): 330 (M^+, 28), 252 (M^+ − Py), 224 (M^+ − COPy, 53), 204 (M^+ − $ClPyCH_2$, 5), 189 (5), 126 (Cl − Py − CH_2, 100). EI-HRMS calcd for $C_{15}H_{11}ClN_4OS$, 330.0342; found 330.0357. Anal. ($C_{15}H_{11}ClN_4OS$) calcd C, 54.46; H, 3.35; N, 16.94; found C, 54.08; H, 3.47; N, 16.86. Compound **3**: yield, 83%; mp = 155 °C. ^{1}H NMR: δ 5.50 (s, 2H), 6.78 (d, 1H, J = 4.8 Hz), 7.07 (d, 1H, J = 4.8 Hz), 7.33 (d, 1H, J = 8.3 Hz), 7.39 (m, 1H), 7.70 (d, 1H, J = 8.3, 2.1 Hz), 8.48 (d, 1H, J = 2.1 Hz), 8.50 (m, 1H), 8.71 (dd, 1H, J = 4.8, 2.0 Hz), 9.51 (d, 1H, 1.4 Hz). ^{13}C NMR: δ 48.9, 110.6, 123.3, 124.9, 125.3, 130.2, 132.0, 136.7, 138.7, 149.1, 151.0, 152.0, 152.2, 168.3, 172.7. EI-LRMS *m*/*z* (%): 330 (M^+, 51), 293 (M^+ − Cl, 44), 224 (M^+ − COPy, 49), 204 (M^+ − $ClPyCH_2$, 44), 188 (16), 126 (Cl − Py − CH_2, 100). EI-HRMS calcd for $C_{15}H_{11}ClN_4OS$, 330.0342; found 330.0343. Anal. ($C_{15}H_{11}ClN_4OS$) calcd C, 54.46; H, 3.35; N, 16.94; found C, 54.19; H, 3.35; N, 16.67. Compound **4**: yield 30%; mp = 179−180 °C. ^{1}H NMR: δ 5.51 (s, 2H), 6.81 (d, 1H, J = 4.6 Hz), 7.10 (d, 1H, J = 4.6 Hz), 7.34 (d, 1H, J = 8.5 Hz), 7.67 (dd, 1H, J = 8.5 Hz, 2.3 Hz), 8.08 (d, 2H, J = 6.3 Hz), 8.48 (d, 1H, J = 2.3 Hz), 8.76 (d, 2H, J = 6.3 Hz). ^{13}C NMR: δ 48.9, 110.9, 122.8, 125.0, 125.5, 130.1, 138.6, 143.8, 149.2, 150.4, 152.1, 168.7, 172.5. EI-LRMS *m*/*z* (%): 330 (M^+, 53), 293 (M^+ − Cl, 11), 224 (M^+ − COPy, 18), 204 (M^+ − $ClPyCH_2$, 12), 189 (15), 126 (Cl − Py − CH_2, 55). EI-HRMS calcd for $C_{15}H_{11}ClN_4OS$, 330.0342; found 330.0334. Anal. ($C_{15}H_{11}ClN_4OS$) calcd C, 54.46; H, 3.35; N, 16.94; found C, 54.42; H, 3.52; N, 16.87. Compound **5**: yield 35%; mp = 249−250 °C. ^{1}H NMR: δ 5.54 (s, 2H), 6.83 (d, 1H, J = 4.8 Hz), 7.10 (d, 1H, J = 4.8 Hz), 7.33 (d, 1H, J = 8.3 Hz), 7.76 (dd, 1H, J = 8.3, 2.2 Hz), 8.49 (d, 1H, J = 2.2 Hz), 8.68 (m, 1H), 8.75 (m, 1H), 9.51 (m, 1H). ^{13}C NMR (DMSO-d_6): δ 48.7, 111.0, 125.0, 128.4, 132.0, 140.4, 145.1, 146.0, 146.8, 149.3, 150.4, 150.5, 168.1, 170.4. EI-LRMS *m*/*z* (%): 331 (M^+, 28), 252 (M^+ − pyrazyl, 55), 224 (M^+ − COpyrazyl, 26), 126 (Cl-pyridyl − CH_2, 100). EI-HRMS calcd for $C_{14}H_{10}ClN_5OS$, 331.0295; found 331.0295. Anal. ($C_{14}H_{10}ClN_5OS$) calcd C, 50.68; H, 3.04; N, 21.11; found C, 50.69; H, 3.35; N, 20.90.

Biology. Radioligand binding experiments involved (1) [^{3}H]IMI with the native *Drosophila* brain nAChR and insect−vertebrate hybrid recombinant receptor consisting of aphid *Myzus* α2 and rat β2 subunits and (2) [^{3}H]nicotine with chick α4β2 nAChR.[13,16,17] Insecticidal activity was evaluated with adult female houseflies via intrathoracic injection and topical application in the absence and the presence of a cytochrome P450 inhibitor [*O*-propyl *O*-(2-propynyl)phenylphosphonate (PPP)], which serves as a synergist by reducing the oxidative detoxification rate.[18] Mosquito larvicidal activities against susceptible (CQ1) and permethrin-resistant (Marin) colonies of *Culex quinquefasciatus* were examined with fourth instars and 24 h of exposure according to McAbee et al.[19] Mammalian toxicity was determined with male albino Swiss-Webster mice (25−30 g) treated intraperitonealy with the test compound dissolved in Me_2SO.

Modeling and Calculations. The X-ray crystal structure for *Aplysia californica* AChBP[6] as the EPI-bound form (PDB code 2BYQ) was used as the template for building the insect nAChR homology model. The protein sequences of the α2 and β1 subunits for *M. persicae*[20,21] obtained from UniProt[22] (accession numbers P91764 for α2 and Q9NFX8 for β1) were aligned with 2BYQ using the CLUSTALW[23] Web server at the European Bioinformatics Institute.[24,25] Chain A of the PDB structure was chosen for sequence alignment with the ligand binding domain (residues α2 1−240 versus 2BYQ:A and β1 1−240 versus 2BYQ:A). These alignments were input to the SWISS-MODEL protein homology server.[26] The resulting model subunit structures were imported into Maestro 7.5 (Schrödinger, L.L.C., Portland, OR). The α2 and β1 model structures were aligned via comparison of backbone atoms onto the corresponding subunits in 2BYQ with further optimization limited to a single α2/β1 subunit pair and hence a single binding interface. This α2β1 model was subjected to cycles of energy minimization using the OPLS_2005 force field implemented in Macromodel 9.1.[27,28] Up to 5000 steps per minimization were run to achieve a gradient of 0.5 with respect to energy. In the initial minimization cycles, the backbone was held constant. In subsequent minimization cycles, the region within 15 Å of the binding pocket was free to move with progressive constraints on the remainder of the structure. Docking calculations were carried out using AutoDock 4.[29,30] The receptor was treated as rigid, while flexible ligands were docked in a 15 Å cubic grid centered on the active site. In each case, a 200 step Lamarkian genetic algorithm search was performed. Good quality hits were those with binding energies below −7 kcal/mol. Selected hits were treated for further MD simulations. These were minimized, then equilibrated for 10−100 ps and simulated for 100 ps to 1 ns at 300 K with a 1 fs time step and SHAKE applied to all bonds to hydrogen. These simulations were run using Macromodel with the OPLS2005 force field and a water continuum model.

Acknowledgment. J.E.C. was supported by the William Muriece Hoskins Chair in Chemical and Molecular Entomology. M.T. and J.E.C. were supported by National Institute of Environmental Health Sciences Grant R01 ES08424, and K.A.D. was supported by National Science Foundation Grant CHE-0233882. The authors received technical assistance from Berkeley colleague Daniel Nomura. Anthony Cornel and Roy McAbee of the Mosquito Control Research Laboratory, Department of Entomology, University of California at Davis, assayed and provided the data for the mosquito larvicidal activity.

Supporting Information Available: Structural models for binding site interactions of compounds **5** and **9** with the *A. californica* AChBP and a table listing elemental analysis results of target compounds. This material is available free of charge via the Internet at http://pubs.acs.org.

References

(1) Tomizawa, M.; Casida, J. E. Selective toxicity of neonicotinoids attributable to specificity of insect and mammalian nicotinic receptors. *Annu. Rev. Entomol.* **2003**, *48*, 339–364.

(2) Tomizawa, M.; Casida, J. E. Neonicotinoid insecticide toxicology: mechanisms of selective action. *Annu. Rev. Pharmacol. Toxicol.* **2005**, *45*, 247–268.

(3) Tomizawa, M.; Talley, T. T.; Maltby, D.; Durkin, K. A.; Medzihradszky, K. F.; Burlingame, A. L.; Taylor, P.; Casida, J. E. Mapping the elusive neonicotinoid binding site. *Proc. Natl. Acad. Sci. U.S.A.* **2007**, *104*, 9075–9080.

(4) Tomizawa, M.; Maltby, D.; Talley, T. T.; Durkin, K. A.; Medzihradszky, K. F.; Burlingame, A. L.; Taylor, P.; Casida, J. E. Atypical nicotinic agonist bound conformations conferring subtype selectivity. *Proc. Natl. Acad. Sci. U.S.A.* **2008**, *105*, 1728–1732.

(5) Celie, P. H. N.; van Rossum-Fikkert, S. E.; van Dijk, W. J.; Brejc, K.; Smit, A. B.; Sixma, T. K. Nicotine and carbamylcholine binding to nicotinic acetylcholine receptors as studied in AChBP crystal structures. *Neuron* **2004**, *41*, 907–914.

(6) Hansen, S. B.; Sulzenbacher, G.; Huxford, T.; Marchot, P.; Taylor, P.; Bourne, Y. Structures of *Aplysia* AChBP complexes with nicotinic agonists and antagonists reveal distinctive binding interfaces and conformations. *EMBO J.* **2005**, *24*, 3635–3646.

(7) Ishimitsu, K.; Kishimoto, T.; Yamada, Y.; Yamada, T.; Takakusa, N. Preparation of (*N*-Heterocyclylimino)heterocyclic Compounds as Insecticides. PCT Int. Appl. WO 92/15564, 1992.

(8) Samaritoni, J. G.; Demeter, D. A.; Gifford, J. M.; Watson, G. B.; Kempe, M. S.; Bruce, T. J. Dihydropiperazine neonicotinoid compounds. Synthesis and insecticidal activity. *J. Agric. Food Chem.* **2003**, *51*, 3035–3042.

(9) Tetko, I. V.; Gasteiger, J.; Todeschini, R.; Mauri, A.; Livingstone, D.; Ertl, P.; Palyulin, V. A.; Radchenko, E. V.; Zefirov, N. S.; Makarenko, A. S.; Tanchuk, V. Y.; Prokopenko, V. V. Virtual computational chemistry laboratory: design and description. *J. Comput.-Aided Mol. Des.* **2005**, *19*, 453–463.

(10) Palmer, C. J.; Casida, J. E. 1-(4-Ethynylphenyl)-2,6,7-trioxabicyclo[2.2.2]octanes: a new order of potency for insecticides acting at the GABA-gated chloride channel. *J. Agric. Food Chem.* **1989**, *37*, 213–216.

(11) Corbel, V.; Duchon, S.; Zaim, M.; Hougard, J.-M. Dinotefuran: a potential neonicotinoid insecticide against resistant mosquitoes. *J. Med. Entomol.* **2004**, *41*, 712–717.

(12) Liu, H.; Cupp, E. W.; Guo, A.; Liu, N. Insecticide resistance in Alabama and Florida mosquito strains of *Aedes albopictus*. *J. Med. Entomol.* **2004**, *41*, 946–952.

(13) Tomizawa, M.; Millar, N. S.; Casida, J. E. Pharmacological profiles of recombinant and native insect nicotinic acetylcholine receptors. *Insect Biochem. Mol. Biol.* **2005**, *35*, 1347–1355.

(14) Tomizawa, M.; Maltby, D.; Medzihradszky, K. F.; Zhang, N.; Durkin, K. A.; Presley, J.; Talley, T. T.; Taylor, P.; Burlingame, A. L.; Casida, J. E. Defining nicotinic agonist binding surfaces through photoaffinity labeling. *Biochemistry* **2007**, *46*, 8798–8806.

(15) Latli, B.; D'Amour, K.; Casida, J. E. Novel and potent 6-chloro-3-pyridinyl ligands for the $\alpha4\beta2$ neuronal nicotinic acetylcholine receptor. *J. Med. Chem.* **1999**, *42*, 2227–2234.

(16) Tomizawa, M.; Zhang, N.; Durkin, K. A.; Olmstead, M. M.; Casida, J. E. The neonicotinoid electronegative pharmacophore plays the crucial role in the high affinity and selectivity for the *Drosophila* nicotinic receptor: an anomaly for the nicotinoid cation$-\pi$ interaction model. *Biochemistry* **2003**, *42*, 7819–7827.

(17) Zhang, N.; Tomizawa, M.; Casida, J. E. Structural features of azidopyridinyl neonicotinoid probes conferring high affinity and selectivity for mammalian $\alpha4\beta2$ and *Drosophila* nicotinic receptors. *J. Med. Chem.* **2002**, *45*, 2832–2840.

(18) Liu, M.-Y.; Lanford, J.; Casida, J. E. Relevance of [^{3}H]imidacloprid binding site in house fly head acetylcholine receptor to insecticidal activity of 2-nitromethylene- and 2-nitroimino-imidazolidines. *Pestic. Biochem. Physiol.* **1993**, *46*, 200–206.

(19) McAbee, R. D.; Kang, K.-D.; Stanich, M. A.; Christiansen, J. A.; Wheelock, C. E.; Inman, A. D.; Hammock, B. D.; Cornel, A. J. Pyrethroid tolerance in *Culex pipiens pipiens var molestus* from Marin County, California. *Pest Manage. Sci.* **2004**, *60*, 359–368.

(20) Sgard, F.; Fraser, S. P.; Katkowska, M. J.; Djamgoz, M. B. A.; Dunbar, S. J.; Windass, J. D. Cloning and functional characterization of two novel nicotinic acetylcholine receptor α subunits from the insect pest *Myzus persicae*. *J. Neurochem.* **1998**, *71*, 903–912.

(21) Huang, Y.; Williamson, M. S.; Devonshire, A. L.; Windass, J. D.; Lansdell, S. J.; Millar, N. S. Cloning, heterologous expression and co-assembly of Mpβ1, a nicotinic acetylcholine receptor subunit from the aphid *Myzus persicae*. *Neurosci. Lett.* **2000**, *284*, 116–120.

(22) Bairoch, A.; Apweiler, R.; Wu, C. H.; Barker, W. C.; Boeckmann, B.; Ferro, S.; Gasteiger, E.; Huang, H.; Lopez, R.; Magrane, M.; Martin, M. J.; Natale, D. A.; O'Donovan, C.; Redaschi, N.; Yeh, L.-S. L. The universal protein resource (UniProt). *Nucleic Acids Res.* **2005**, *33*, D154−D159.

(23) Thompson, J. D.; Higgins, D. G.; Gibson, T. J. CLUSTALW: improving the sensitivity of progressive multiple sequence alignment through sequence weighting, position-specific gap penalties and weight matrix choice. *Nucleic Acids Res.* **1994**, *22*, 4673–4680.

(24) Lassmann, T.; Sonnhammer, E. L. L. Kalign, an accurate and fast multiple sequence alignment algorithm. *BMC Bioinf.* **2005**, *6*, 298.

(25) Lassmann, T.; Sonnhammer, E. L. L. Kalign, Kalignvu and Mumsa: Web servers for multiple sequence alignment. *Nucleic Acids Res.* **2006**, *34*, W596−W599.

(26) Schwede, T.; Kopp, J.; Guex, N.; Peitsch, M. C. SWISS-MODEL: an automated protein homology-modeling server. *Nucleic Acids Res.* **2003**, *31*, 3381–3385.

(27) Mohamadi, F.; Richard, N. G. J.; Guida, W. C.; Liskamp, R.; Lipton, M.; Caufield, C.; Chang, G.; Hendrickson, T.; Still, W. C. Macromodel, an integrated software system for modeling organic and bioorganic molecules using molecular mechanics. *J. Comput. Chem.* **1990**, *11*, 440–467.

(28) Jorgensen, W. L.; Maxwell, D. S.; Tirado-Rives, J. Development and testing of the OPLS all-atom force field on conformational energetics and properties of organic liquids. *J. Am. Chem. Soc.* **1996**, *118*, 11225–11236.

(29) Morris, G. M.; Goodsell, D. S.; Halliday, R. S.; Huey, R.; Hart, W. E.; Belew, R. K.; Olson, A. J. Automated docking using a Lamarckian genetic algorithm and an empirical binding free energy function. *J. Comput. Chem.* **1998**, *19*, 1639–1662.

(30) Huey, R.; Morris, G. M.; Olson, A. J.; Goodsell, D. S. A semiempirical free energy force field with charge-based desolvation. *J. Comput. Chem.* **2007**, *28*, 1145–1152.

JM800191A